

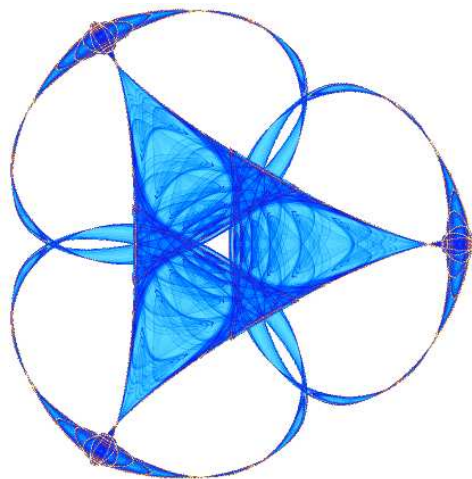
**GRADIENT-BASED IMAGE FUSION FOR  
HDR CREATION IN DYNAMIC SCENES**

By

**Sira Ferradans**  
**Marcelo Bertalmío**  
**Edoardo Provenzi**  
and  
**Vicent Caselles**

**IMA Preprint Series # 2370**

(June 2011)



**INSTITUTE FOR MATHEMATICS AND ITS APPLICATIONS**

UNIVERSITY OF MINNESOTA  
400 Lind Hall  
207 Church Street S.E.  
Minneapolis, Minnesota 55455-0436

Phone: 612-624-6066 Fax: 612-626-7370  
URL: <http://www.ima.umn.edu>

# Gradient-based Image Fusion for HDR creation in dynamic scenes

Sira Ferradans, Marcelo Bertalmío, Edoardo Provenzi and Vicent Caselles

**Abstract**—In this paper we will tackle the problem of HDR image generation for dynamic scenes. The current techniques assume the scene to be static in order to create the radiance map. Otherwise, strong artifacts appear. Some attempts have been made to extend these methods directly to dynamic scenes, but, as we will explain, an intensity fusion approach leads to spatial inconsistencies in the radiance values. We propose a gradient-based approach that avoids bleeding and ghosting, two common artifacts. Moreover the method improves the detail rendition of the original images. To support the validity of our method, results and comparisons with the state of the art will be presented.

## I. INTRODUCTION

Outdoor scenes are usually very contrasted and their radiance can span several orders of magnitude, but regular commercial cameras can only produce low dynamic range (LDR) photographs which capture two orders of magnitude, so they can be affected by saturated areas and loss of contrast and detail. High Dynamic Range (HDR) images have become very popular in the last ten years mostly because they allow to render more detailed scenes which are closer to human perception. HDR image creation techniques assume that the input images are in perfect alignment and there is no motion,

otherwise artifacts will appear. These assumptions make outdoor scenes, handheld camera photographs and HDR images of living subjects very difficult to produce. For a thorough overview of the HDR imaging we refer the interested reader to the excellent book by Reinhard et al [1]

In this paper we present a method for HDR image creation from LDR images with motion, based on fusion techniques. A common approach to image fusion is an *image stitching* perspective: the final image is created by copying pieces of images from a sequence [2], [3]. However, this approach can lead to inconsistencies in the final image. If we consider scenes with large motion, the final image will easily be incoherent, with duplication of objects. Moreover, errors due to the camera function estimation, noise or aliasing present in the radiance maps will be reproduced.

Instead of synthesizing a new image from the sequence, we are interested in the scenario where the user wants to increase the dynamic range of a photograph (the *reference image*) from a stack of pictures of the same scene.

The contribution of this paper is the following: given a set of differently exposed LDR images of a dynamic scene, with camera and/or object motion, we

propose an algorithm which is able to create an HDR version of the reference image, with improve detail rendition. The results compare well with the state of the art, not showing common artifacts called color bleeding or ghosting [4], [2]. Color bleeding is an artifact that appears to the viewer as the diffusion of artificial color over a flat region while ghosting appears as a translucent element present in another image of the sequence.

## II. STATE OF THE ART IN HDR CREATION FOR DYNAMIC SCENES

Most methods in the state of the art have mainly three steps: *inversion of the camera function* (also referred to as radiometrical alignment [2]), *motion detection* and *fusion*.

For registered static scenes, the motion estimation and image fusion steps are straight-forward: all pixels are already aligned so fusion can be done with a weighted average. Thus the problem lies on how to estimate the camera function  $f$ . This problem was first stated by Mann and Picard [5] who assumed  $f$  to be concave. Debevec and Malik [6] relax the constraint assuming  $f$  to be smooth and propose a numerical method that has become the standard for static scenes. Mitsunaga and Nayar approximate  $f$  as a polynomial function [7]. A thorough analysis of the camera function space was developed by Grossberg and Nayar [8] who also propose a method based on histograms, thus more robust to motion [9].

Regarding dynamic scenes, both the registration of LDR images with different exposure time and the creation of an

artifact-free radiance map are open problems. In the state of the art, methods generally focus on one of these two issues. Regarding image registration, Ward [10] proposes to use multi-scale techniques to register a set of Median Threshold Maps (MTB), which are a binarization of the images with respect to their median value. Although this approach is independent of the exposure time it depends on the noise and histogram density around the median value. Grosch [11] bases a local registration method on these MTBs and Jacobs et al. [12] propose an improvement by estimating motion with an entropy based descriptor. These methods give good results for hand held camera scenarios with no motion in the scene but tend to produce artifacts when dealing with large object motion (e.g. such as people walking through the scene.) Tomaszewska and Mantiuk [13] and Heo et al. [14] propose to compute a global homography using RANSAC with SIFT descriptors which are based on gradients, thus independent of exposure time. Finally, Kang et al. [15] propose to use the camera function to boost the original images in order to facilitate the registration process.

On the other hand we have a group of methods that focus mainly on the fusion step. In dynamic scenes, if we assume a perfect correspondence among pixels and perform a weighted time average of radiances, artifacts called *ghosts* appear in the areas with motion. The methods in the state of the art called *ghost free methods* focus on not creating ghosts by reducing the influence of motion pixels in the final fused image. These methods generally assume a previous image alignment step. The most common approach, which

we call *intensity fusion approach*, is to fuse the image radiances by a properly weighted average. Khan et al. [16] and Heo et al. [14] propose a weight that depends on how likely a pixel is to belong to the foreground. Granados et al. [17] define a weight with optimal statistical results assuming a compound-Gaussian noise. Grosch [11] and Jacobs et al. [12] average only those pixels that belong to the background.

The methods based on intensity fusion can be robust to pixel saturation and small misalignments, but the areas that appear only in one image will be *copied* while the other image areas are *averaged* from different images, thus new boundaries can be created. In order to deal with these artifacts, Gallo et al. [4] propose to use Poisson-based techniques. They create a vector field by copying patches of gradients from the best exposed areas that match a reference image. Then they blend the borders of neighboring patches and integrate the vector field. The resulting images are ghost free but artifacts appear on the patch borders and flat regions.

Gradient-based methods can deal with the radiance differences among the image sequence but are sensitive to misalignments and can produce color bleeding as Eden et al. [2] have reported.

### III. AN OVERVIEW OF THE PROPOSED ALGORITHM

The proposed method improves the detail rendition of a reference image using a stack of images taken with different exposure time. The first step is to apply the inverse camera function to every image obtaining a radiance map for each one. These radiance maps are

radiometrically aligned using the camera function and the exposure value of the reference image. These modified images are used to compute a dense correspondence field (using the optical flow algorithm of Chambolle and Pock [18]) of every image in the stack with the reference image. These correspondences are filtered using a Refinement step based on modeling the histogram of (absolute value of) motion compensated image differences of every pair of images as a mixture of Gaussians. Finally, we use the corrected correspondences to obtain a gradient field that we integrate by solving the Poisson equation. To avoid color bleeding and other color artifacts we set a randomly selected group of points as Dirichlet boundary conditions. The intensity values of these points are computed through intensity fusion.

### IV. INTENSITY FUSION

Let us start by introducing the intensity fusion problem as first presented by Mann and Picard [5]. We consider a set of  $N$  static LDR images  $X_j : \Omega \rightarrow [0, \dots, 255]$  where  $j = 1, \dots, N$  of area  $\Omega$  taken with exposure time  $\Delta t_j$ , respectively. Thus, for every point  $\mathbf{x} = (x_0, y_0)$ ,  $X_j(\mathbf{x})$  is a generic intensity level that will be specify further on. The goal is to obtain the radiance value  $E(\mathbf{x})$  which is ideally given by the equation:

$$E_j(\mathbf{x}) = \frac{f^{-1}(X_j(\mathbf{x}))}{\Delta t_j}, \quad (1)$$

where  $f^{-1}$  is the inverse of the camera function.<sup>1</sup> In theory, all radiance images

<sup>1</sup>In this paper we assume the camera function to be known because it can be precomputed from static images. There are several methods to estimated  $f$ , we use the one proposed by Debevec and Malik [6].

$E_j$  should be equivalent, but in practice when applying  $f^{-1}$  to several images  $X_j$  of the same scene the computed radiance  $E_j$  can change in orders of magnitude due to noise in the original image, aliasing and errors in the estimation of the camera function. Moreover, the camera function  $f$  is not linear but saturates in the extrema of the LDR losing details in the dark and bright areas. Thus the radiance map  $E_j$  depends on the LDR image  $X_j$  and its exposure time. We can attenuate errors and introduce details in the over/under exposed areas by averaging the radiance maps of each LDR image in the following way:

$$E(\mathbf{x}) = \sum_{j=0}^N w_j(X_j(\mathbf{x})) \frac{f^{-1}(X_j(\mathbf{x}))}{\Delta t_j}, \quad (2)$$

where  $w_j$  is a weighting function.

This method gives excellent results when all pixels  $X_j(\mathbf{x})$  are perfectly aligned. Otherwise *ghosts* appear. Therefore a registration step of the reference image with the images in the sequence is needed.

## V. REGISTRATION

The goal of our method is to create a HDR version of the reference image with increased detail rendition, that is to say, in the areas where the reference image is over/under exposed we want to introduce the detail present in other images of the stack, without creating artifacts produced by merging motion pixels. Thus we need to compute optical flow among the reference image and each of the other images in the sequence. That is to say, we need to decide for every pair pixels

whether they were produced by the same object in the scene and therefore can be fused together, or if one of them is a motion pixel and has to be ignored in the fusion process. An important issue arises when comparing two images: how to distinguish motion pixels that we do not want to fuse from details that are not present in the reference image, but appear in other images of the set, that we indeed want to fuse. Comparing directly radiance values will make undistinguishable both cases, lost details and motion, and the same would happen if we compare normalized gradients. Moreover, the difference among the radiance maps will produce a lot of false positives.

It is worth noticing that these differences cannot be circumvented reducing the range, using for example a logarithmic scale. The differences in the radiance maps come from the differences among the original LDR images: low-key images get their noise amplified by the inverse camera function, high-key images render properly the dark areas but have no detail on the bright areas. These features will not come closer together by any function that is not the camera function itself. Thus we propose a radiometric modification of each radiance map by applying the camera function with the same exposure time (the one of the reference image). The intensity levels become closer and the areas of the images from the set that correspond to the saturated areas of the reference image will also appear saturated. We have empirically observed that matching the histogram [19] of each radiometrically aligned image to the reference image histogram improves results.

Once the radiance maps have been ra-

diometrically aligned we can apply any optical flow (OF) method over the new LDR images. We propose to use the method by Chambolle and Pock [18]. Given two images (reference image and an image from the set), this method gives dense correspondences among pixels. Although the matchings are accurate, it can produce errors on the boundaries of moving objects and the areas where objects disappear due to motion. A refinement step is needed to check whether the correspondences are correct or not.

#### A. Refinement

Let us assume we have two radiometrically aligned images  $\bar{X}_{\text{ref}}, \bar{X}_j$  without motion. The pixelwise distance between them  $\|\bar{X}_{\text{ref}}(\mathbf{x}) - \bar{X}_j(\mathbf{x})\|$  will depend on the noise of both images. If we model this noise as additive and Gaussian, the difference image histogram will be highly densed close to zero. As the motion (or mismatches) among the images increases, more modes will appear in this histogram. Thus we propose to model this difference histogram as a set of Gaussians using a Gaussian Mixture Model (GMM) where the most probable Gaussian is associated to the properly matched pixels and the other Gaussians represent those matchings that are not correct. Let the most probable gaussian be defined as  $\mathcal{N}(\mu, \sigma)$ , we define as a mismatch those correspondences with a distance above  $\mu + \alpha\sigma$ , where  $\alpha$  is a parameter of the algorithm. Although in theory the value of  $\mu$  should be zero, in practice it is not and it must be estimated.

## VI. GRADIENT FUSION

In this paper, we are assuming the general case where the image stack has

subjects that move and are occluded in time. Let us point out that the most common situation when creating the final HDR map will be the case where we do not have correspondences for all pixels of the reference image to pixels in all the other images of the set. Thus averaging different numbers of pixel intensities (corresponding to a pixel of the reference image) will create artificial edges, given that the radiance maps  $E_j$  have noticeable radiance differences. In order to avoid these problems we propose to use gradient fusion techniques in the log-scale  $\tilde{E}_j = \text{Log}(E_j)$ .

In 2003, Perez et al. [20] introduced a method called *Poisson Editing* which allowed seamless cloning, that is to say, to modify the features of an image without creating new edges or artifacts. The idea is to modify the gradient field of the image inside a certain area  $\Omega^M \subset \Omega$  by copying the gradient field of some other image, creating a vector field that is integrated by solving the Poisson equation.

The main advantage of this method with respect to other image editing tools is that the new features are introduced inside  $\Omega^M$  but matching the colors at the boundary of  $\Omega^M$ , thus illumination changes over the new areas are also simulated.

The goal of our method is to improve the detail rendition of the final image, that is to say, in the fusion process we want to give more importance to those gradients with largest norm. On the other hand, we know that our radiances  $\tilde{E}_j$  may differ in orders of magnitude due to noise, aliasing, saturation, etc. thus their gradients will also differ in magnitude and direction. We propose to combine the corresponding gradients in a robust way, as it is com-

only done in the fusion literature [21].

The idea is to obtain for every pixel the predominant gradient within the image sequence. To do so, let us define the weighted second moment matrix as:

$$G_s(\mathbf{x}) = \begin{pmatrix} \sum_{j=0}^N s_j^2(\mathbf{x}) \left(\frac{\partial \tilde{E}_j}{\partial x}\right)^2 & \sum_{j=0}^N s_j^2(\mathbf{x}) \frac{\partial \tilde{E}_j}{\partial x} \frac{\partial \tilde{E}_j}{\partial y} \\ \sum_{j=0}^N s_j^2(\mathbf{x}) \frac{\partial \tilde{E}_j}{\partial y} \frac{\partial \tilde{E}_j}{\partial x} & \sum_{j=0}^N s_j^2(\mathbf{x}) \left(\frac{\partial \tilde{E}_j}{\partial y}\right)^2 \end{pmatrix} \quad (3)$$

where  $\nabla \tilde{E}_j = \left(\frac{\partial \tilde{E}_j}{\partial x}, \frac{\partial \tilde{E}_j}{\partial y}\right)$  is the gradient of  $\tilde{E}_j$  and  $s_j(\mathbf{x}) = \frac{\|\nabla \tilde{E}_j(\mathbf{x})\|}{\left(\sum_{i=1}^N \|\nabla \tilde{E}_i(\mathbf{x})\|^2\right)^{1/2}}$ . The largest eigenvector of matrix  $G_s$  is the predominant direction of the gradients and the corresponding eigenvalue is its norm. In this process the sign is lost. In our experiments, we have seen that using the sign of the largest gradient gives good results.

Given the pixel  $\mathbf{x}$ , in the reference image, we define  $M(\mathbf{x})$  as the gradient of the pixel corresponding to  $\mathbf{x}$  with maximum modulus. Then, the target vector in pixel  $\mathbf{x}$  is defined as:

$$V(\mathbf{x}) = \sqrt{\lambda} \varepsilon(\mathbf{x}) \theta \quad (4)$$

where  $\lambda$  is the largest eigenvalue of  $G_s(\mathbf{x})$ ,  $\theta$  its associated eigenvector and  $\varepsilon(\mathbf{x})$  is defined as:

$$\varepsilon(\mathbf{x}) = \begin{cases} -1 & \text{if } \theta M(\mathbf{x}) \leq 0 \\ 1 & \text{otherwise.} \end{cases}$$

Poisson Editing can also be understood as the minimization of the following energy:

$$\int_{\Omega^M} |\nabla \tilde{E}(\mathbf{x}) - V(\mathbf{x})|^2 d\Omega^M. \quad (5)$$

The solution  $\tilde{E}^*(\mathbf{x})$  will have a gradient field as close as possible to  $\mathbf{V}$ . The difference between  $\mathbf{V}$  and  $\nabla \tilde{E}^*$  is called the *residual error* and depends on how close is  $\mathbf{V}$  to a conservative field. The

residual error is responsible for the bleeding effect along strong edges reported by Tao et al. [22] which becomes crucial on HDR images. Eden et al. [2] have also reported problems when using Poisson Editing tools for HDR images.

Thus, we have a vector field  $\mathbf{V}$  that may have small errors that when accumulated can produce bleeding artifacts. To stop this accumulation we propose to set some Dirichlet boundary conditions inside the image, i.e. some fixed pixel values with known valid radiances. A priori we have no information to set these boundary values given that we do not know where the errors will accumulate, but we know they can appear in any part of the image. Thus, we randomly distribute the Dirichlet points along all the image area. The second problem is which radiance value should these points have. The reference image may lack reliable colors in many parts of the image due to saturation and so would any image in the stack. But we know that an appropriate color can be obtained from averaging pixel values through the image set. We propose to select from these randomly distributed pixels those that are not motion pixels, i.e. those pixels from the reference image that have correspondences in the images of the stack, and average them using eq. (2).

## VII. ALGORITHM AND IMPLEMENTATION

Now that the method has been described we can proceed to give some implementation details. The optical flow method of Chambolle and Pock [18] was applied over the luminance values of the radiometrically aligned images, and the

number of Gaussians for the GMM was two. A final step in the refinement process is introduced to avoid pixels on the boundaries: understanding the mismatches as motion masks, we apply a dilation morphological filter with a structuring element of radius six pixels [19]. In the fusion process we randomly select 10% of the total image area as possible Dirichlet points keeping only those with matches. The intensity of these Dirichlet points is defined using eq. (2) where  $w_j(X_j(\mathbf{x})) = \exp\{-(X_j(\mathbf{x}) - 127)^2 / (2\sigma^2)\}$ . Setting  $\sigma$  to 30 gives good results. Finally, we solve the Poisson equation using the Conjugate Gradient method [23] for each color channel independently.

### VIII. RESULTS AND COMPARISONS

HDR images cannot be represented on a LDR display, so to show the results obtained from our algorithm we will show different simulated exposure times obtained with the HDRShop software [24]. The comparison with the state of the art will be done following the procedure used in other papers, that is, using tone mapping.

#### A. Results

Let us start by showing the improvement obtained using our method. In Fig. 2 we can see the original radiance maps compared to the output we obtain. All radiance maps are shown in HDRShop. The change is specially obvious on the building where it recovers texture and color, as can be seen also on the detail presented in Fig. 1. In this case, the sky appears clearer in the processed image. The images on

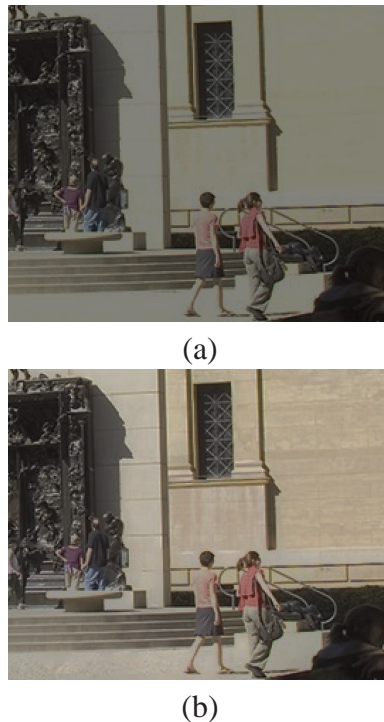


Fig. 1. Detail of the Garden image (a) original radiance map (b) radiance map obtained with our algorithm. Both shown with HDRShop.

the second row of Fig. 2 show the same images at a higher exposure time. Notice, in particular that the tree on the left hand side of the processed image shows much more details than the original one. All these images were obtained setting  $\alpha$  to 1.

1) *Parameter  $\alpha$* : The algorithm has one parameter  $\alpha$  that controls the flexibility in the correspondences selection. The range that we have observed that gives good results is  $[0.5, 1]$ , being 0.5 more conservative. Not setting correctly this parameter may create artifacts, as can be seen in Fig. 4.

2) *Influence of the reference image selection*: The selection of the reference image can also influence the appearance of



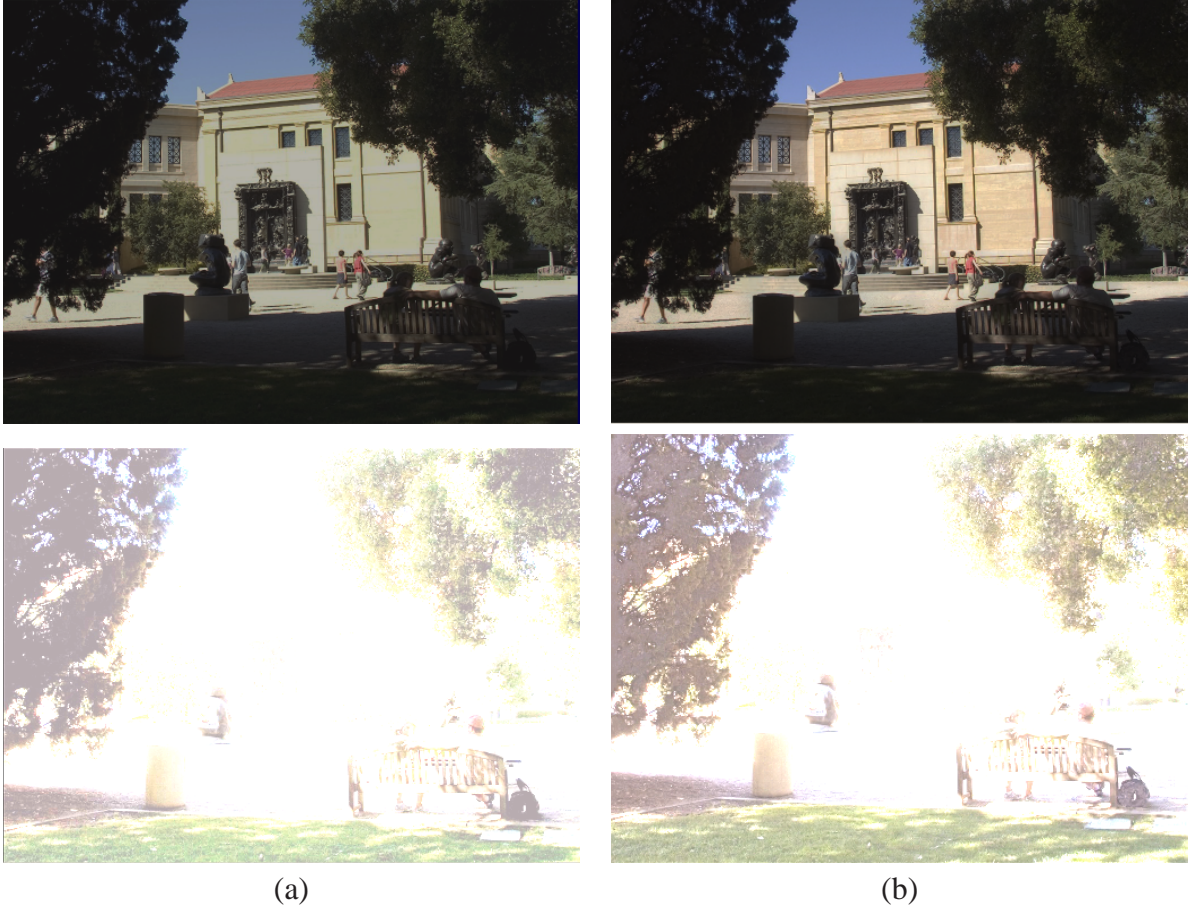


Fig. 2. (a) Original image (b) Output generated by our algorithm, for more details see text.

ghosts or artifacts. The correspondences selection depends on the differences between the radiometrically aligned images. We have observed that when a moving pixel with a color similar to the background is located in an area saturated by the camera function, the Refinement step may fail to distinguish background from foreground, thus color artifacts may appear. We can see an example in Fig. 3, in the first row we present two images of the stack that were used as a reference image. The corresponding results are shown in the row below. In both cases the parameter value is  $\alpha = 1$ .

Note that the result presented on the left hand side has an artifact on the puppet's leg. Since the reference image is saturated in that area, the puppet's leg and the ball cannot be distinguished by the Refinement step.

#### B. Comparison with the state of the art

In this section we will compare our results with Gallo et al.'s method [4]. They present their results using an interactive Tone Mapping technique proposed by Lischinski et al. [25]. Instead we will use the tone mapping method proposed by Ferradans et al. [26] for our results.

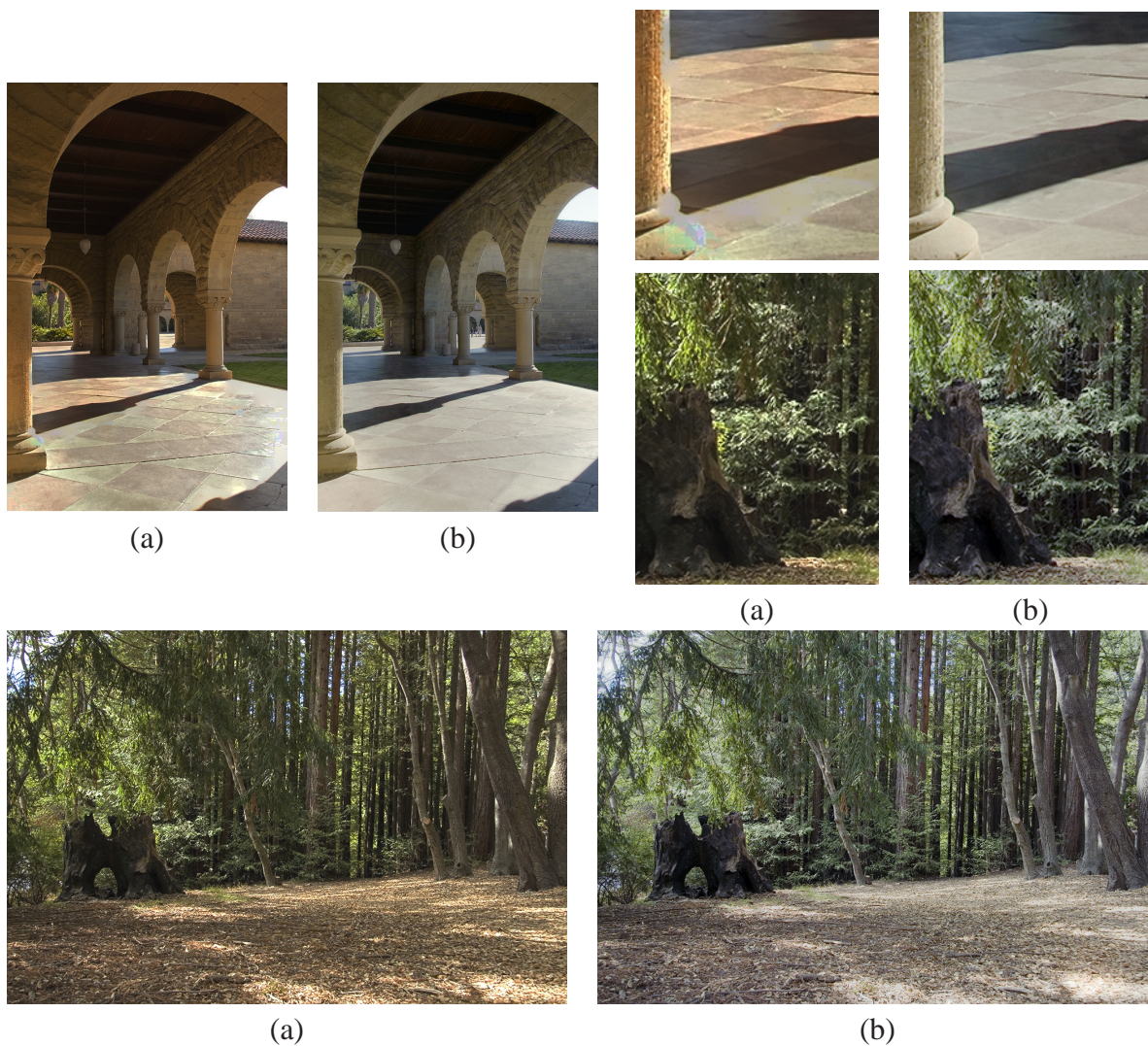


Fig. 5. (a) Original image (b) Output generated by our algorithm

In Fig. 5, the results obtained with Gallo et al.'s and the proposed method can be compared. In both images our method gives coherent results without bleeding, color or geometric artifacts, as can be seen in the general images as well as the provided details. Apart from the absence of artifacts, we would like to stress that the color of the tiles is homogeneous along all the floor, and does not change

across the column shadows.

## IX. CONCLUSIONS AND FUTURE WORK

We have proposed a method for HDR image creation on dynamic scenes based on gradient fusion techniques that compares well to the state of the art. We have proposed a new method for motion detection by modeling the difference histogram as a mixture of Gaus-



Fig. 3. In the first row we can see the original LDR images used as the reference image. The second row shows the output of our algorithm.



Fig. 4. A more conservative value of parameter  $\alpha$  avoids color artifacts. Results obtained using  $\alpha$  set to (a) 1 (b) 0.5.

sians. We have pointed out the importance of using gradient-based method instead of intensity-based methods and gave a solution to the usual bleeding problems that appear when integrating vector fields. Finally, we would like to remark that although this method can give good results, the obtained images were constrained by the ISO value, being always set to lower values such as 80,100 or 200 in order to avoid noise. As a future work we propose to introduce a de-noising step that would allow us to use LDR images with higher

ISO, making the whole capture process faster.

## X. ACKNOWLEDGEMENTS

The authors would like to thank O. Gallo for kindly providing his images.

## REFERENCES

- [1] E. Reinhard, G. Ward, S. Pattanaik, and P. Debevec, *High Dynamic Range Imaging, Acquisition, Display, And Image Based Lighting*. San Francisco, USA: Morgan Kaufmann Ed, 2005.
- [2] A. Eden, M. Uyttendaele, and R. Szeliski, "Seamless image stitching of scenes with large motions and exposure differences," in *Computer Vision and Pattern Recognition, 2006 IEEE Computer Society Conference on*, vol. 2, 2006, pp. 2498 – 2505.
- [3] M. Granados, H.-P. Seidel, and H. P. A. Lensch, "Background estimation from non-time sequence images," in *Graphics Interface*, 2008, pp. 33–40.
- [4] O. Gallo, N. Gelfand, W. Chen, M. Tico, and K. Pulli, "Artifact-free high dynamic range imaging," *IEEE International Conference on Computational Photography (ICCP)*, April 2009.
- [5] S. Mann and R. W. Picard, "On being undigital with digital cameras: Extending dynamic range by combining differently exposed pictures," in *Proceedings of IS&T*, 1995, pp. 442–448.
- [6] P. Debevec and J. Malik, "Recovering high dynamic range radiance maps from photographs," in *Proc. of the 24th annual conf. on Computer graphics*, 1997, pp. 369–378.
- [7] T. Mitsunaga and S. Nayar, "Radiometric self calibration," in *Computer Vision and Pattern Recognition, 1999. IEEE Computer Society Conference on.*, vol. 1, 1999, pp. –380 Vol. 1.
- [8] M. Grossberg and S. Nayar, "Modeling the Space of Camera Response Functions," *IEEE Transactions on Pattern Analysis and Machine Intelligence*, vol. 26, no. 10, pp. 1272–1282, Oct 2004.
- [9] M. D. Grossberg and S. K. Nayar, "Determining the camera response from images: What is knowable?" *IEEE Trans. Pattern Anal. Mach. Intell.*, vol. 25, no. 11, pp. 1455–1467, 2003.
- [10] G. Ward, "Fast, robust image registration for compositing high dynamic range photographs from handheld exposures." *Journal of graphic tools*, vol. 8, pp. 17–30, 2003.
- [11] T. Grosch, "Fast and robust high dynamic range image generation with camera and object movement," in *Vision, Modeling and Visualization, RWTH Aachen*, 2006, pp. 277–284.

- [12] K. Jacobs, C. Loscos, and G. Ward, "Automatic high-dynamic range image generation for dynamic scenes," *IEEE Computer Graphics and Applications*, vol. 28, pp. 84–93, 2008.
- [13] A. Tomaszewska and R. Mantiuk, "Image registration for multi-exposure high dynamic range image acquisition," in *Proc. Intl. Conf. Central Europe on Computer Graphics, Visualization, and Computer Vision (WSCG)*, 2007. [Online]. Available: [http://wscg.zcu.cz/wscg2007/Papers\\_2007/fullB13-full.pdf](http://wscg.zcu.cz/wscg2007/Papers_2007/fullB13-full.pdf)
- [14] Y. Heo, K. Lee, S. Lee, Y. Moon, and J. Cha, "Ghost-free high dynamic range imaging," in *Computer Vision - ACCV 2010*, ser. Lecture Notes in Computer Science, R. Kimmel, R. Klette, and A. Sugimoto, Eds. Springer Berlin-Heidelberg, 2011, vol. 6495, pp. 486–500.
- [15] S. B. Kang, M. Uyttendaele, S. Winder, and R. Szeliski, "High dynamic range video," *ACM Trans. Graph.*, vol. 22, pp. 319–325, July 2003. [Online]. Available: <http://doi.acm.org/10.1145/882262.882270>
- [16] E. Khan, A. Akyuz, and E. Reinhard, "Ghost removal in high dynamic range images," in *Image Processing, 2006 IEEE International Conference on*, oct. 2006, pp. 2005–2008.
- [17] M. Granados, B. Ajudin, M. Wand, C. Theobalt, H.-P. Seidel, and H. Lensch, "Optimal hdr reconstruction with linear digital cameras," in *Computer Vision and Pattern Recognition (CVPR), 2010 IEEE Conference on*, june 2010, pp. 215–222.
- [18] A. Chambolle and T. Pock, "A first-order primal-dual algorithm for convex problems with applications to imaging," *Journal of Mathematical Imaging and Vision*, vol. 40, no. 1, pp. 120–145, 2011.
- [19] R. Gonzales and R. Woods, *Digital image processing*. Prentice Hall, 2002.
- [20] P. Pérez, M. Gangnet, and A. Blake, "Poisson image editing," in *ACM SIGGRAPH 2003 Papers*, ser. SIGGRAPH '03. New York, NY, USA: ACM, 2003, pp. 313–318.
- [21] G. Piella, "Image fusion for enhanced visualization: A variational approach," *International Journal of Computer Vision*, vol. 83, pp. 1–11, 2009, 10.1007/s11263-009-0206-4. [Online]. Available: <http://dx.doi.org/10.1007/s11263-009-0206-4>
- [22] M. W. Tao, M. K. Johnson, and S. Paris, "Error-tolerant image compositing," in *Proceedings of the 11th European conference on Computer vision: Part I*, ser. ECCV'10. Berlin, Heidelberg: Springer-Verlag, 2010, pp. 31–44.
- [23] J. R. Shewchuk, "An introduction to the conjugate gradient method without the agonizing pain," Pittsburgh, PA, USA, Tech. Rep., 1994.
- [24] [Online]. Available: <http://www.hdrshop.com/>
- [25] D. Lischinski, Z. Farbman, M. Uyttendaele, and R. Szeliski, "Interactive local adjustment of tonal values," in *SIGGRAPH '06: ACM SIGGRAPH 2006 Papers*. New York, NY, USA: ACM, 2006, pp. 646–653.
- [26] S. Ferradans, M. Bertalmio, E. Provenzi, and V. Caselles, "An analysis of visual adaptation and contrast perception for tone mapping," *Pattern Analysis and Machine Intelligence, IEEE Transactions on*, vol. PP, no. 99, p. 1, 2011.